LA-4754-MS
C. 1

Some Preliminary Numerical Studies
of Taylor Instability
Which Include Effects of Material Strength

los alamos
scientific laboratory
of the University of California
LOS ALAMOS, NEW MEXICO 87544

This report, like other special-purpose documents in the LA. . .MS series, has not been reviewed or verified for accuracy in the interest of prompt distribution.

los alamos
scientific laboratory
of the University of California
LOS ALAMOS, NEW MEXICO 87544

Some Preliminary Numerical Studies
of Taylor Instability
Which Include Effects of Material Strength

by

K. A. Meyer
P. J. Blewett

SOME PRELIMINARY NUMERICAL STUDIES OF TAYLOR INSTABILITY
WHICH INCLUDE THE EFFECTS OF MATERIAL STRENGTH

by

K.A. Meyer and P.J. Blewett

ABSTRACT

In this numerical study a two-dimensional Lagrangian code, TOODY II, is used to compute the growth of a perturbed interface between a perfect gas and an aluminum plate. The interface undergoes acceleration in the direction of the gas to the aluminum. Using an elastic perfectly plastic model for the aluminum the effects of yield strength, density ratio, wavelength, initial amplitude, and the elastic shear modulus on the perturbation growth rate are presented. Results are compared with Taylor theory and an attempt is made to develop an analytic expression for the effect of yield strength.

NOTATION

P   pressure

ρ density

E   specific internal energy

Γ Gruneisen constant

U   shock speed

u   particle speed

S^{ij} stress deviator tensor

w^{ij} spin tensor, $w^{ij} = \frac{1}{2}\left(\frac{\partial u^i}{dx^j} - \frac{\partial u^j}{\partial x^i} \right)$

G   elastic modulus of shear

σ^{ij} stress tensor

ϵ^{ij} strain rate deviator tensor

Y^o yield strength in tension

η perturbation amplitude

λ perturbation wavelength

a   acceleration

ν Poisson's ratio

c_o "bulk" sound speed

I. INTRODUCTION

During the course of a combined numerical and experimental investigation of Taylor instability in aluminum plates (to be published) some questions arose as to the relative effects of material strength, density ratio, wavelength and initial perturbation size on the growth of the disturbance. A series of numerical test problems with a much simpler configuration than the actual experimental flow was considered in order to obtain some qualitative information. The results of these preliminary numerical studies are presented here.

The configuration under consideration is given in Fig. 1 and consists of a perfect gas at an initial pressure of .1 Mb, density of .55 gm/cm^3 with an adiabatic exponent $\gamma = 3$ and an aluminum plate also at a pressure of .1 Mb and with a density of 3.14 gm/cm^3. The gas and plate extend indefinitely in the y direction. The right face of the aluminum is held at zero pressure while the left boundary of the gas is kept at .1 Mb. The gas-aluminum interface has a half sine wave perturbation with wavelength λ and initial amplitude η_o.

As the rarefaction proceeds into the aluminum from the right the plate is accelerated. When the rarefaction crosses the interface we have the case of a perturbed interface being accelerated in the direction of low to high density, which in the clas-

sical incompressible fluid case is unstable. Because of the wave action we have a time varying acceleration. The variation of the interface pressure with time (averaged over a wavelength λ) is given in Fig. 2. Figure 3 is a plot of the average gas density (over a wavelength) adjacent to the interface versus time while Fig. 4 is the density-time plot for the aluminum next to the interface. The time origin for these problems is 2.34 µsec; i.e., the rarefaction commences at the free surface of aluminum at t = 2.34 µsec.

II. PHYSICAL MODEL OF ALUMINUM PLATE

The code used in these calculations is TOODY II,[1] a two-dimensional Lagrangian code developed at Sandia Corporation. Here we will briefly describe the physical model used for the stress supporting aluminum plate. The "hydro" equation of state $P(\rho,E)$ is the conventional Mie-Gruneisen equation for the pressure P off the Hugoniot,

$$P - P_H = \rho\Gamma(E-E_H) , \qquad (1)$$

where the subscript H indicates Hugoniot values. For the linear fit of shock speed versus particle speed,

$$U = c_o + su , \qquad (2)$$

Eq. (1) implies,

$$P = P_H \left\{ 1 - \frac{\Gamma}{2}\left(\frac{\rho}{\rho_o} - 1\right) \right\} + \Gamma\rho E , \qquad (3)$$

where,

$$P_H = \frac{\rho_o c_o^2 \, \alpha(\alpha-1)}{[(s-1)\alpha-s]^2} , \qquad (4)$$

$$\alpha = \frac{\rho}{\rho_o} . \qquad (5)$$

The values used for the above constants were:

$\rho_o = 3.14$ gm/cm^3

$c_o = 0.535$ cm/µsec

$s = 1.35$

$\Gamma = 1.70$

In addition to the hydrodynamic character of the aluminum an elastic component is appended by

differencing the following equations:

$$S^{xx} - 2w^{xz} S^{xz} = 2G\left[\frac{\partial u^x}{\partial x} + \frac{1}{3}\frac{1}{\rho}\frac{\partial\rho}{\partial t}\right] \qquad (6)$$

$$S^{xz} + w^{xz}(S^{xx}-S^{zz}) = G\left[\frac{\partial u^x}{\partial z} + \frac{\partial u^z}{\partial x}\right] \qquad (7)$$

$$S^{zz} + 2w^{xz} S^{xz} = 2G\left[\frac{\partial u^z}{\partial z} + \frac{1}{3}\frac{1}{\rho}\frac{\partial\rho}{\partial t}\right] \qquad (8)$$

$$S^{yy} = -(S^{xx}+S^{zz}) . \qquad (9)$$

By definition the stress deviators, S^{ij}, indicate how much a normal stress deviates from the average of the three normal stresses, which by definition is the pressure,

$$S^{ij} = \sigma^{ij} + P\delta^{ij} , \qquad (10)$$

$$P = -\frac{1}{3}(\sigma^{xx}+\sigma^{yy}+\sigma^{zz}) . \qquad (11)$$

Equations (6) through (8) are derived in reference 2. They consitute an extension of Hooke's law from static elasticity to dynamics. The effect of the second term on the left-hand side of these equations is to take into account the fact that a rigid body rotation changes the tensor components, S^{ij}. That is, under a rigid body rotation Hooke's law in the static equilibrium sense would say that the stress deviators would not change because there is no deformation of shape. The equations of conservation of momentum, however, require the stress deviator components on the fixed (x,z) frame. Thus the stress deviator components must be "corrected" for any rigid body motion occurring within the time step, Δt. If one then ignores the rotation terms in Eqs. (6) through (8) he will see that what remains is an identification of a stress rate deviator with the appropriate strain rate deviator, i.e., Hooke's law differentiated with respect to time. Of course the above equations are transformed to Lagrangian coordinates in TOODY; we have left them in Eulerian form for purposes of interpretation.

After finding all $(S^{ij})^{n+1}$ by means of Eqs. (6) through (9) (all quantities on the right-hand side are known at $n+\frac{1}{2}$ from momentum equations) we first find the second invariant of the stress deviator tensor, $\phi/2$, where,

$$\dot{\tau}^{n+1} = [(S^{xx})^2 + (S^{yy})^2 + (S^{zz})^2 + 2(S^{xz})^2]^{n+1}.$$

$$(12)$$

We then use the von-Mises criterion to test whether

$$\phi^{n+1} \leq \frac{2}{3}(Y^0)^2 , \qquad (13)$$

where Y^0 is the yield strength in tension. If condition (13) holds, the values of $(S^{ij})^{n+1}$ found from Eqs. (6) through (9) are considered the "true values" and the medium is described as "elastic." If condition (13) is violated all we can conclude is that at some intermediate time within $\Delta t = t^{n+1} - t^n$ plastic flow has occurred and therefore, Eqs. (6) through (9) did not apply over the complete interval. One interpretation of the von-Mises criterion is that there is an upper limit to the energy of distortion (as opposed to the work done in changing the volume) that the medium can absorb. When this limit is reached the medium can support only this disparity in the stress deviators regardless of the strains. See references 3 and 4 for fuller discussions of the von-Mises criterion. Over Δt then the total strain has now an unknown elastic strain component and a plastic strain component. There are various theories such as the Prandtl-Reuss theory and the von-Mises theory that relate the plastic strain rate component to stress; however, all the theories demand that in the plastic regime the equality in Eq. (13) must be maintained for the so-called perfectly plastic model. Wilkins shows in reference 3 that a method, consistent with the von-Mises flow rule which in our notation may be written as,

$$S^{ij} = \frac{Y^0}{3 \text{ II}} \dot{\epsilon}_p^{ij} , \qquad (14)$$

(here $\dot{\epsilon}_p^{ij}$ is the plastic component of the strain rate deviator and II is the second invariant of that tensor) is to reduce each $(S^{ij})^{n+1}$ found from Eqs. (6) through (9) in proportion to the extent the von-Mises criterion is violated, i.e.,

$$(S^{ij})^{n+1} \rightarrow \sqrt{\frac{\frac{2}{3}(Y^0)^2}{\phi^{n+1}}}(S^{ij})^{n+1} \qquad (15)$$

C. Mader has calibrated dynamic yield strengths for aluminum based on one-dimensional experiments by J.

Taylor using a model similar to the above.[5] Suffice it to say that there is a wealth of models covering elastic, plastic, and viscous behavior of materials and until definitive experiments can be made it seems prudent to choose the very simplest model.

III. DISCUSSION

Before discussing the numerical data it is of interest to ascertain the rate of perturbation growth from classical incompressible theory using an average acceleration and representative densities.

The average acceleration of the system of the gas and aluminum plate can be obtained as follows. The initial conditions are

$$\tau_{A\ell} = .254 \text{ cm} \quad (\text{A}\ell \text{ plate thickness})$$

$$\tau_{gas} = .356 \text{ cm}$$

$$\rho_{A\ell} = 3.14 \text{ gm/cm}^3$$

$$\rho_{gas} = .55 \text{ gm/cm}^3$$

while the total pressure drop is .1 Mb, therefore the average acceleration is

$$a = \frac{P}{\rho_{A\ell}\tau_{A\ell} + \rho_{gas}\tau_{gas}} = .101 \text{ cm/}\mu\text{sec} . \qquad (16)$$

This implies an average interface pressure

$$P_i = a \times \rho_{A\ell}\tau_{A\ell} = .081 \text{ Mb} \qquad (17)$$

which is in reasonable agreement with what one obtains from the numerical solution as represented by Fig. 2.

From the classical linear incompressible theory we have

$$\eta = \eta_0 \ell^{\alpha t} , \qquad (18)$$

where η is the perturbation amplitude and where

$$\alpha = \sqrt{\frac{2\pi}{\lambda} a \frac{\rho_{A\ell} - \rho_{gas}}{\rho_{A\ell} + \rho_{gas}}} = \frac{d \ln \eta}{dt} . \qquad (19)$$

The question arises as to what are the relevant densities to use in Eq. (18). Two sets of densities were tried; first the initial densities $\rho_{gas} = .55$ gm/cm^3 and $\rho_{A\ell} = 3.14$ gm/cm^3 , and second, estimated averages obtained from Figs. 3 and 4, namely $\rho_{gas} = .505$ gm/cm^3 and $\rho_{A\ell} = 3.06$ gm/cm^3. Table 1 lists the linear incompressible values of $d \ln \eta/dt$

3

for the cases of interest. These will be compared later to the numerical results.

Numerical problems were run with an initial gas density of .55 gm/cm^3 and an aluminum density of 3.14 gm/cm^3. Aluminum yield strengths of 0.0, 1.0, 2.0, and 3.0 Kb were considered as were shear moduli of 93 Kb, 280 Kb and 839 Kb. The effect of density ratio was investigated by replacing the .55 gm/cm^3 gas by a vacuum and using a time varying applied pressure profile obtained from Fig. 2. Perturbation wavelengths of .254 cm and .508 cm were considered as were initial amplitudes of .01016 cm and .02032 cm.

The growth of the perturbation with time is given in Figs. 5 through 8. Figure 5 is for an initial perturbation amplitude of .02032 cm and a wavelength of .508 cm. The "gas" density was zero, that is an applied pressure profile was prescribed on the left surface of the aluminum. The aluminum had a shear modulus of 280 Kb and curves for yield strengths of 0.0, 1.0, 2.0 and 3.0 Kb are included. Figure 6 is for the same conditions as Fig. 5 but an initial gas density of .55 gm/cm^3 was used. Figure 7 conditions duplicate those of Fig. 6 but the perturbation wavelength was changed to .254 cm. Figure 8 conditions differ from those in Fig. 7 only in that the initial perturbation was .01016 cm (rather than .02032 cm). All of these plots (Figs. 5 - 8) show that after a relatively short initial period the perturbation grows exponentially. The rates of growth, $d \ln \eta/dt$, obtained from the graphs (slopes of the straight lines on the figures) are tabulated in Table I. For the case of 0.0 Kb yield strength the numerical growth rates can be compared with those obtained from Eq. (19) for linear incompressible theory. One can see immediately that the numerically obtained values of $d \ln \eta/dt$ are always lower than the linear incompressible results. Furthermore, the ratio of the numerical to linear results for λ = .254 cm is not the same as that for λ = .508 cm hence there is a wavelength dependence in the function relating the numerical solution to the linear approximation. The data indicate that for the no strength case the growth rate is not dependent on the amplitude of the initial perturbation (in the range considered).

It would appear that the rather large periodic oscillations of pressure and density at the interface

have an effect on the perturbation growth rate and simply trying to use time averages of these quantities in the linear theory is not sufficient to give agreement with the numerical calculations. This means we have no simple analytic model against which to judge the effect of changing variables (e.g., o, λ, η_0) and hence since the numerical data is rather sparse we can only get qualitative results. We do see that increasing yield strength results in decreasing the rate of growth. Also halving the wavelength increases the rate of growth $d \ln \eta/dt$ (but not by the $\sqrt{2}$ as would be predicted by Eq. (19) for zero yield strength). Reducing the initial amplitude has negligible effect on the low strength cases (0.0 and 1.0 Kb yield strength) but has a marked effect at higher yield strength (2.0 and 3.0 Kb). If we define the Atwood ratio as

$$\delta = \frac{\rho_{Al} - \rho_{gas}}{\rho_{Al} + \rho_{gas}} , \qquad (20)$$

then for the applied pressure (vacuum) case δ = 1, whereas for the gas case ρ_{gas} = .55 gm/cm^3 and ρ_{Al} = 3.14 so we have δ = .7. From Table I we see that the reduction in growth rate associated in going from a base flow δ = 1, λ = .508 cm, η_0 = .02032 cm and 0.0 yield strength to the same flow but with δ = .7 is the same as the reduction obtained by going from the base flow to one with the only change being yield strength, namely a yield of 2.0 Kb instead of zero.

An attempt was made to try to determine a model which would indicate more clearly the effect of yield strength. We consider an expression (analogous to Eq. (19)) of the form

$$\frac{d \ln \eta}{dt} = \alpha = \sqrt{\frac{2\pi}{\lambda} a \frac{\rho_{Al} - \rho_{gas}}{\rho_{Al} + \rho_{gas}} - H(Y^0, \lambda, o,)} \quad .(21)$$

If we assume that $H(Y^0 = 0)$ = 0 and define

$$A^2 = \sqrt{\frac{2\pi}{\lambda} a \frac{\rho_{Al} - \rho_{gas}}{\rho_{Al} + \rho_{gas}}} = \frac{d \ln \eta}{dt} \bigg|_{Y^0 = 0} . \qquad (22)$$

Then $\alpha = A^2 - H$. If we take A from the zero yield strength calculation in Table I and look at H as a function of yield strength we can obtain curves of H vs. yield strength. These curves are plotted in Figs. 9 and 10 and indicate that H is a linear function of yield strength.

A further feature of the strength model used

in the code is shown by the data in Table II. Here we have kept λ, η_0, and yield strength constant and varied the shear modulus G. The wide variation in G (a factor of 9 from the largest to the smallest values of G considered) produced no variation in the rate of growth of the perturbation.

REFERENCES

1. L. Bertholf and S. Benzley, "TOODY II: A Computer Program for Two-Dimensional Wave Propagation," Sandia Laboratories, SC-RR-68-41 (November 1968).

2. A. Eringen, *Nonlinear Theory of Continuous Media* (McGraw-Hill, Inc., New York, 1962).

3. M. Wilkins, "Calculation of Elastic-Plastic Flow," Lawrence Radiation Laboratory, UCRL-7322, Rev. 1, (January 1969).

4. W. Prager and P. Hodge, *Theory of Perfectly Plastic Solids* (John Wiley and Sons, New York, 1951).

5. C. L. Mader, "One-Dimensional Elastic-Plastic Calculations for Aluminum," Los Alamos Scientific Laboratory, LA-3678 (February 1967).

Fig. 1.   Typical initial configuration for a gas-aluminum problem with perturbation wavelength λ.

TABLE I

$\frac{d \ln \eta}{dt}$ from Numerical Runs

here λ = .508 cm and η_0 = .02032 cm

Problem Description	Y^0 = 0. Kb	Y^0 = 1.0 Kb	Y^0 = 2.0 Kb	Y^0 = 3.0 Kb
Vac, λ, η_0	1.010	.933	.864	.782
Gas, λ, η_0	.847	.765	.668	.565
Gas, $\lambda/2$, η_0	1.145	.972	.782	.595
Gas, $\lambda/2$, $\eta_0/2$	1.137	.948	.657	.454
Linear Theory-Vac, λ, η_0	1.118	Numerical/linear = $\frac{1.010}{1.118}$ = .905		
Linear Theory-Gas, λ, η_0				
a) Initial Densities	.936	Numerical/linear = $\frac{.847}{.936}$ = .905		
b) Average Densities	.945	Numerical/linear = $\frac{.847}{.945}$ = .896		
Linear Theory-Gas, $\lambda/2$, η_0				
a) Initial Densities	1.324	Numerical/linear = $\frac{1.145}{1.324}$ = .865		
b) Average Densities	1.336	Numerical/linear = $\frac{1.145}{1.336}$ = .857		

TABLE II

Effect of Shear Modulus on Perturbation Growth Rate

Y^0 = 1.0 Kb. Initial Bulk Modulus $K_0 = \rho_0 c_0^2$, for all cases

G = .093 Mb ν = .450		G = .280 Mb ν = .359		G = .859 Mb ν = .144	
t (usec)	η (cm)	t (usec)	η (cm)	t (usec)	η (cm)
2.349	.02032	2.349	.02032	2.349	.02032
2.746	.02061	2.746	.02059	2.740	.02054
3.142	.02681	3.142	.02677	3.143	.02677
3.543	.03348	3.543	.03340	3.542	.03336
3.942	.04241	3.943	.04228	3.940	.04219
4.344	.05674	4.344	.05655	4.344	.05658
4.745	.07506	4.745	.07473	4.746	.07455
5.145	.11069	5.145	.11035	5.141	.10966
5.541	.14568	5.540	.14507	5.541	.14477
5.779	.17362	5.784	.1734	5.781	.17262

Fig. 2.   Gas-aluminum interface pressure vs. time for three cases Y_0 = 1.0 Kb, Y_0 = 2.0 Kb and Y_0 = 3.0 Kb. The pressure is averaged over one perturbation wavelength λ (λ = .508 cm).

5
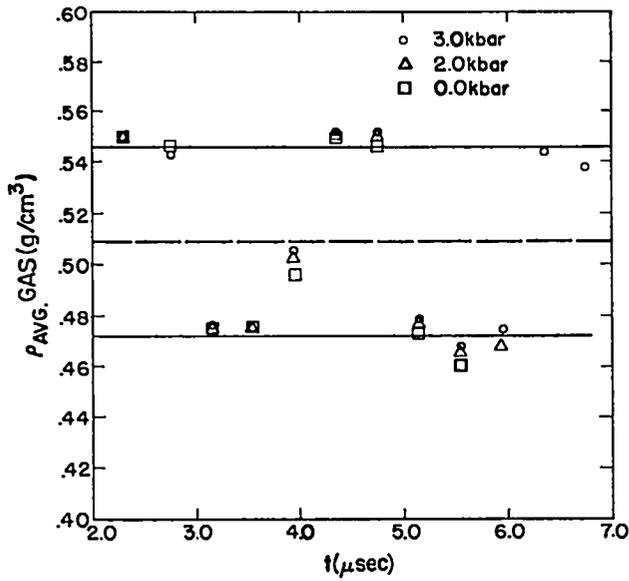
Fig. 3. Gas density adjacent to the perturbed aluminum interface vs. time for the cases Y_o = 0.0 Kb, Y_o = 2.0 Kb and Y_o = 3.0 Kb. The density is averaged over one perturbation wavelength λ (λ = .508 cm).
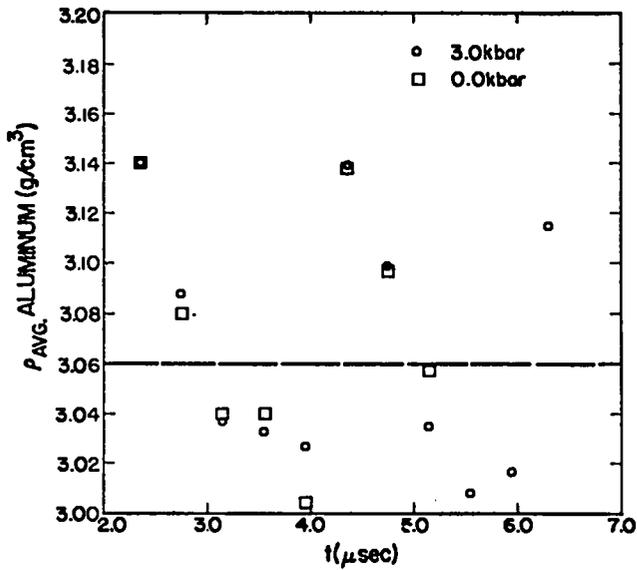
Fig. 4. Aluminum density adjacent to the perturbed interface vs. time for the cases Y_o = 0.0 Kb, Y_o = 2.0 Kb and Y_o = 3.0 Kb. The density is averaged over one perturbation wavelength λ (λ = .508 cm).
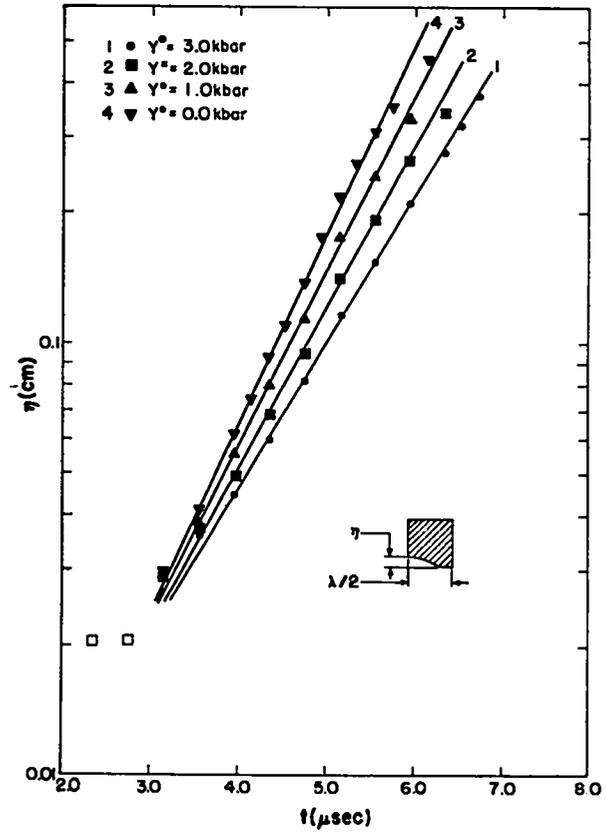
Fig. 5. Perturbation growth for the case of an applied pressure on the aluminum plate. The initial perturbation amplitude η_o = .02032 cm and the wavelength λ = .508 cm. Aluminum yield strengths of 0.0, 1.0, 2.0 and 3.0 Kb are considered.

6
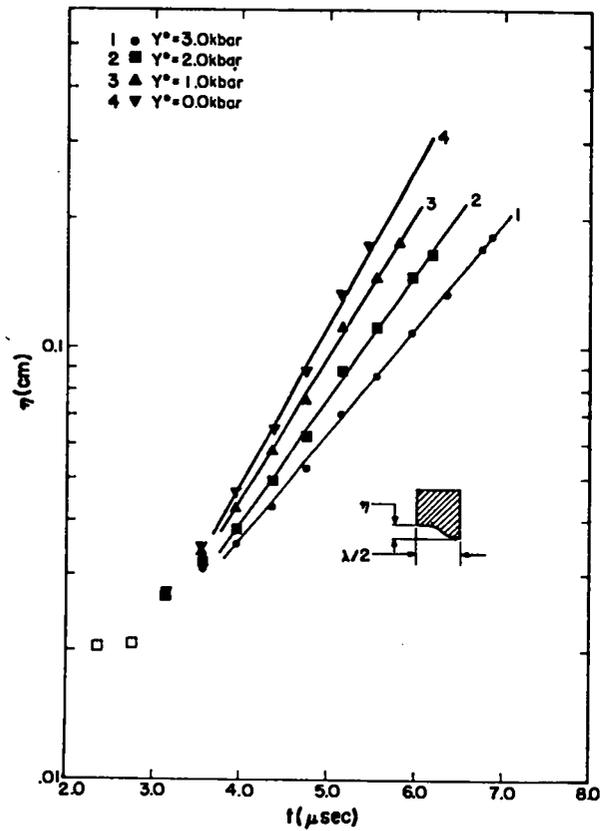
Fig. 6. Perturbation growth for the case of a gas-propelled aluminum plate with initial perturbation amplitude η_o = .02032 cm and wavelength λ = .508 cm. Aluminum yield strength of 0.0, 1.0, 2.0 and 3.0 Kb are considered.
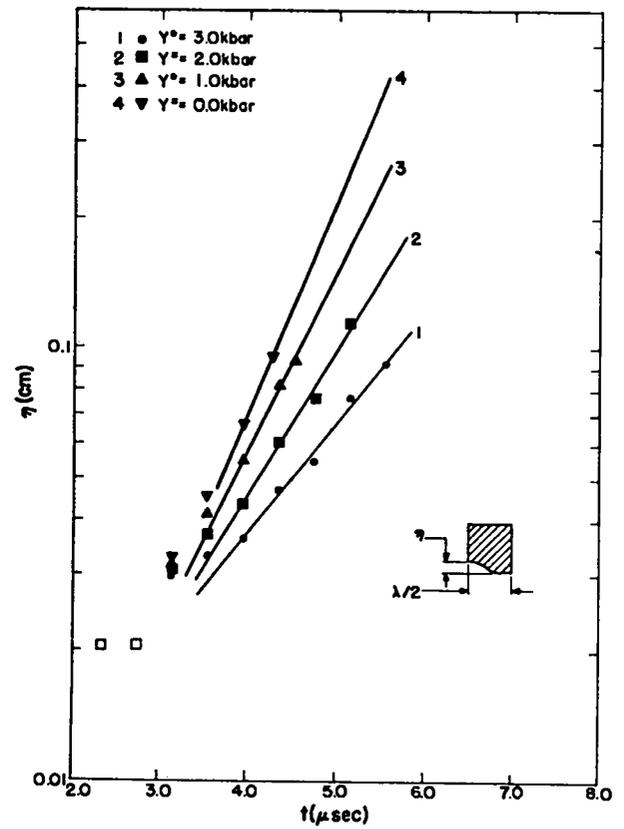
Fig. 7. Perturbation growth for the case of a gas-propelled aluminum plate with an initial perturbation amplitude η_o = .02032 and wavelength λ = .254 cm. Aluminum yield strengths of 0.0, 1.0, 2.0 and 3.0 Kb are considered.
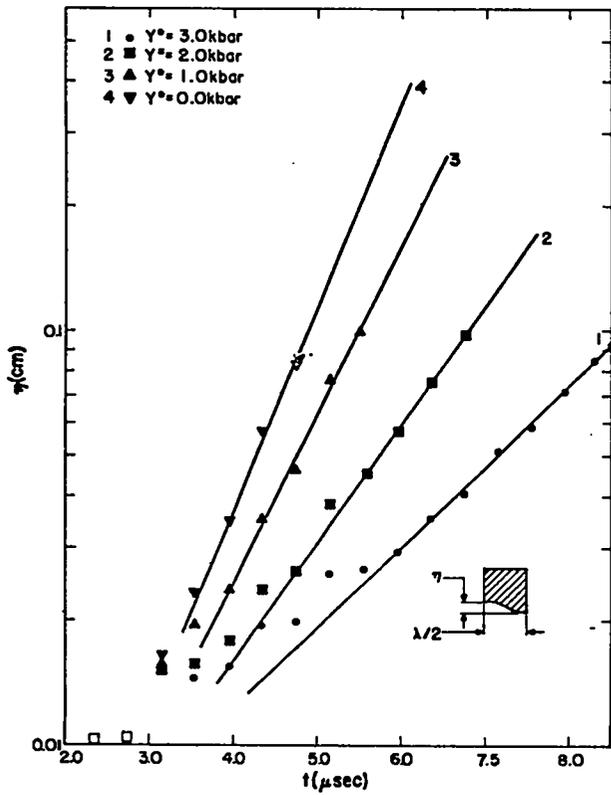
Fig. 8. Perturbation growth for the case of a gas-
propelled aluminum plate with an initial
perturbation amplitude η_o = .01016 and
wavelength λ = .254 cm. Aluminum yield
strengths of 0.0, 1.0, 2.0 and 3.0 Kb are
considered.
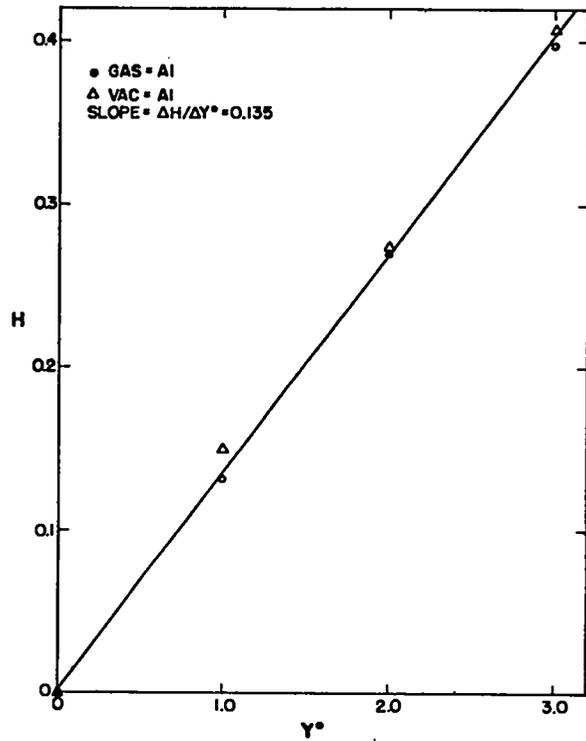
Fig. 9. Plot correlating yield strength Y_o and the
function H (Eq. (21)) for cases with
η_o = .02032 cm and λ = .508 cm.
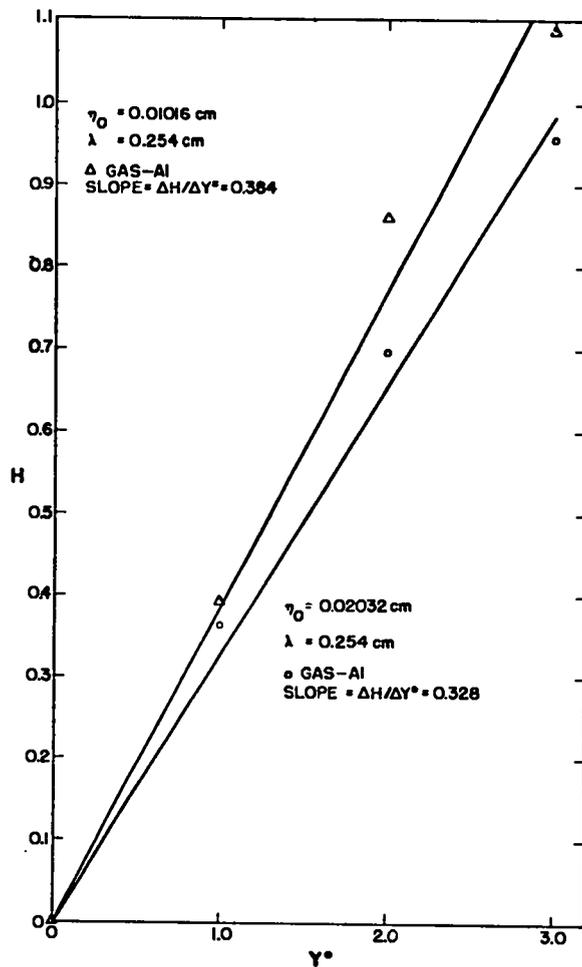
Fig. 10. Plot correlating yield strength Y_o and
the function H (Eq. (21)) for the cases
with η_o = .02032 cm and λ = .254 cm and
the cases with η_o = .01016 cm and λ =
.254 cm.

9